

Burning Skin Detection System in Human Body

Noor M. Abdulhadi, Noor A. Ibraheem and Mokhtar M. Hasan

Department of Computer Science, College of Science for Women, University of Baghdad,
Baghdad, Iraq

Abstract—Early accurate burn depth diagnosis is crucial for selecting the appropriate clinical intervention strategies and assessing burn patient prognosis quality. However, with limited diagnostic accuracy, the current burn depth diagnosis approach still primarily relies on the empirical subjective assessment of clinicians. With the quick development of artificial intelligence technology, integration of deep learning algorithms with image analysis technology can more accurately identify and evaluate the information in medical images. The objective of the work is to detect and classify burn area in medical images using an unsupervised deep learning algorithm. The main contribution is to developing computations using one of the deep learning algorithm. To demonstrate the effectiveness of the proposed framework, experiments are performed on the benchmark to evaluate system stability. The results indicate that, the proposed system is simple and suits real life applications. The system accuracy was 75%, when compared with some of the state-of-the-art techniques.

Index Terms—Skin burn, Clustering, Deep learning, Fuzzy c-means clustering, Image segmentation, Medical images.

I. INTRODUCTION

It is possible to make an accurate diagnosis of burns in the early stages through computerized image processing. The differences in the degree of color between the affected and uninjured skin are the real criterion for distinguishing between them and for knowing the severity of the injury. Distinguishing the type of injury is based on the color analysis method according to criteria and statistical indications to find out the type of injuries if they are mild, moderate, or serious. This technique can be adapted to assess and track wound severity in humans in a clinical setting (Hao, et al., 2021). Regardless of this aspect, this review is for the burned skin area. Whereas different burn areas have different types of burns, the depth of the burn is usually maximum in a burn area. However, a series of tests can be carried out to determine the extent of humidity. An evaluation by a dermatologist after the examination cannot

be ruled out. Expert opinions remain to date the most reliable assessment of injury (Malini, Siva, and Niranjana, 2013). An overview of recent techniques for burn images is presented in (Domagoj and Damir, 2020). This research proposed an artificial intelligence system that uses unsupervised deep learning, to examine the affected area and recognize it, as well as to give an accurate diagnosis.

The skin is the largest organ in the body and is mostly damaged during burn accidents. The skin accounts for 15% of the total weight of an adult human being. The primary functions of the skin are protection, sensation, temperature regulation, and Vitamin D synthesis. The main components of human skin are the epidermis and dermis. The epidermis is the thin outer part of the skin, whereas the dermis is the inner thick layer of connective tissue made of elastic fibers. Burns are characterized by their size, area, and depth. Burns are classified as first-, second-, third-degree, or fourth-degree depending on how deeply and severely they penetrate the skin's surface (Tina, et al., 2015; Kuan, et al., 2018).

A. First-degree (Superficial) Burns

First-degree burns influence just the epidermis, or external layer of skin. The consume site is red, difficult, dry, and without any rankles. Gentle burn from the sun is a model. Long-term tissue harm is uncommon and as a rule comprises an increment or decline in the skin tone (Papini, 2004; Miller, et al., 1998), as shown in Fig. 1.

B. Second-degree (Partial Thickness) Burns

Second-degree burns include the epidermis and a piece of the dermis layer of skin. The consumption site seems red, rankled, and might be enlarged and painful (Hao, et al., 2021; Papini, 2004). Fig. 2 is an example of partial thickness burns.

C. Third-degree (Full Thickness) Burns

Third-degree burns devastate the epidermis and dermis. Third-degree burns may likewise harm the hidden bones, muscles, and ligaments. The affected site seems white or burned. There is no sensation nearby since the sensitive spots are obliterated. Fig. 3 is an example of full-thickness burns.

The rest of the paper is organized as follows. Related work is presented in Section II. Section III introduced proposed system methodology. The experimental results and comparisons with other systems were demonstrated in Section IV. Section V concluded the paper by supplying a summary of the steps taken in this study.





Fig. 1. Superficial dermal burn.



Fig. 2. Partial thickness burn.



Fig. 3. Full thickness burn.

II. RELATED WORKS

The current standard for evaluating burn wounds is based on digital photography of wounds examined by a burn specialist. Researchers are developing automated burn wound analysis systems due to the subjectivity of this approach. These systems should include three major components: burn image segmentation, feature extraction (Hasan, Ibraheem and Abdulhadi, 2022), and classification of segmented regions into healthy skin, and burned skin. (Liu, et al., 2021) introduced a review of some common ideas and characteristic features of medical image segmentation based on deep learning algorithms by applying the segmentation method for different human organs areas such as brain tumors, lung

nodules, eyes, chest, heart, abdomen, and some other parts besides, whereas (Liangrui, Zhichao and Shaoliang, 2022) reviewed an investigation on various methods in pathology in a pathological and technical perspective.

According to the study results, image acquisition type has a significant impact on segmentation and classification performance. The fuzzy c-means algorithm for segmentation and a multilayer feed-forward ANN trained by the back-propagation algorithm for classification were found to be the best combination for successfully categorizing the images into the skin, burn, and background regions (Ugur, et al., 2019).

The deep learning-based image segmentation method achieves excellent results, for example, in (Badrinarayanan, Kendall, and Cipolla, 2017), researchers compared the performance of the segmentation approach versus deep learning, SegNet-based segmentation process was implemented as a deep learning approach (Badrinarayanan, Kendall, and Cipolla, 2017). Mask R-CNN is a method for utilizing the cutting-edge deep learning framework, researchers have modified the Mask R-CNN to adapt the dataset for more refined result and faster training speed (Chong, et al., 2019) (Prabhakar, Gauraveand and Kailesh, 2020). Over-redundant vocabulary is used to detect and classify burnt areas using sparse representations of feature vectors. Feature vectors are extracted from image patches and assigned to a class representing a burning degree for each patch. Color and texture information are used as features (Brenda and Roberto, 2021). Various segmentation algorithms have been proposed to improve classification performance, to extract the wound from an image, the DNN is trained to segment the testing data (Fangzhao, et al., 2018). Authors (Hao, et al., 2021), built a framework that segmented the burn area in burn images and calculated the percentage of burn area in total body surface area (TBSA) to extend the network output structure and label the burn dataset. The framework is then applied to segment multiple burn depth areas. The most important step in image classification is feature extraction. As a result, many works proposed various types of color and/or texture-based features. Alcalá-Fdez, and Alonso (2016) gave a survey of fuzzy systems software in means of taxonomy, recent researchers issues. The features generated by (Deepak, Antony, and Niranjan 2012) are the mean and (2, 1) the coefficient of the discrete cosine transform (DCT) function of the V1 chrominance plane of the $L^*a^*b^*$ color space were extracted as features. Fully convolutional networks (FCN) have been applied by (Despo, et al., 2017), whereas researchers in (Sabeena and Raj Kumar, 2019) have improved the feature extraction of GLCM and further to the SVM method. An automated system for categorizing healthy and burned skin in images of trauma patients was developed. A database was created using 105 images gathered from Turkish burn centers. The effects of color spaces and feature matrices on the results of segmentation-based classification methods were investigated. The FCM algorithm for segmentation and a multilayer feed forward ANN trained by the back-propagation algorithm for classification were found to be the best combination for successfully classifying

burn images. The a^* and b^* channels of the $L^*a^*b^*$ color space were used as input to the FCM algorithm, whereas the artificial neural network was trained using selected Haralick features. The average F-score obtained was 0.7428. Deep learning semantic segmentation was also used to classify burn images. The architecture trained on 64 pixel sized blocks analyzed from training datasets achieved an F-score of 0.805 (Ugur, et al., 2019). Fuzzy c means algorithm based on morphological reconstruction was applied by (Rahman and Islam, 2021), whereas researchers in (Wang, et al., 2021) incorporated a residual-related regularization term derived from the distribution properties of various types of noise into FCM. An image mining approach was used to conduct a comparative study of various classification algorithms on the classification of different burn depths as explained in (Kuan, et al., 2018), authors (Hansen, et al., 1997) developed several approaches for noninvasive burn evaluation in humans in a clinical environment employing a color imaging system for monitoring and tracking wound severity, In (Nameirakpam, Khumanthem, and Yambem, 2015), authors applied K-means clustering algorithm with a subtractive clustering algorithm to segment 5 images. A comprehensive overview of current deep learning-based medical picture segmentation approaches is presented by (Liu, et al., 2021). Wagh, et al., (2020) used smartphone wound picture analysis as a practical tool to monitor the healing process and give patients and caregivers useful feedback in between visits to the hospital.

III. SYSTEM METHODOLOGY

The main objective of this study is to segment different kinds of medical burn images using deep learning. The training and testing set of images were used in their entirety without cropping or any preprocessing detection of the main injured area. Manual input images, and (Stephen, 2020) database has also been used in our work (Health Encyclopedia Site).

The following subsections explain briefly Fuzzy C-means, deep learning algorithm, and proposed work.

A. Fuzzy C-mean Clustering (FCM)

Fuzzy C-means (FCM) is the most widely used approach for pixel categorization. The layout of partition space for clustering algorithms is as follows:

Let c be an integer, and $x_1, x_2, x_3, \dots, x_n$ signify a set of n unlabeled vectors in the space R^p , where p is the number of features in each vector. The standard FCM objective function for partition $(x_k)_{k=1}^n$ into c clusters is given by equations (1), (2), and (3):

$$\text{Minimize } j_m(U, v) = \sum_{k=1}^n \sum_{i=1}^c (u_{ik})^m (d_{ik})^2 \quad (1)$$

$$\text{Subject to } \sum_{j=1}^c u_{ik} = 1, 1 \leq i \leq n \quad (2)$$

$$u_{ik} \geq 0, 1 \leq i \leq n, 1 \leq j \leq c \quad (3)$$

The exponent $m > 1$ is used to adjust the membership value's weighting impact. Where $d_{ik} = \|x_k - v_i\|$. U is the fuzzy partition matrix, which provides the membership of each cluster's feature vectors (Bezdek, 1981) (Bekir, 2016) (Yeganejou and Dick, 2018).

The cluster center matrix is denoted by the letter v , $\{v_1, v_2, \dots, v_c\}$ where v_i is a cluster center of features. The updated cluster center v_i can be obtained from the following equations (4), (5) and (6):

$$v_i = \frac{\sum_{k=1}^n u_{ik}^m x_k}{\sum_{k=1}^n u_{ik}^m} \text{ for each } i \quad (4)$$

The objective function U can be derived from:

$$u_{ik} = \frac{1}{\sum_{j=1}^c \left(\frac{d_{ik}}{d_{jk}}\right)^{\frac{2}{m-1}}} \text{ for each } i \text{ and } k \quad (5)$$

$$u_{ik} = \begin{cases} 1 & \text{if } d_{ik} = 0 \\ 0 & \text{otherwise} \end{cases} \quad (6)$$

In the FCM clustering algorithm, as demonstrated in Fig. 4, each cluster's data points are represented with a different color, and each cluster's center is represented with a black X. For all feature vectors, the cluster center matrix, v , is randomly initialized, and the fuzzy partition matrix U is constructed. The main FCM algorithm's outline is explained as follows:

ALGORITHM: FUZZY PARTITIONING MATRIX U CONSTRUCTION

Input: Feature vectors
Output: Partition matrix U
Data: Initialize cluster center matrix, v . Set $k = 0$.
Begin
Step 1: Initialize the fuzzy clustering matrix, U ($k = 0$) with (5), (6), m is set to be 2.0.
Step 2: Increment $k=k+1$. Compute v using step 3.
Step 3: Compute $U(k)$ using step 4.
Step 4: If $\ U(k) - U(k-1)\ < \epsilon$ then stop, else repeat steps from 1 to 4.
End

B. Deep Learning

Deep learning (DL) is a type of machine learning and training that uses a significant quantity of data to create an informed model. It is one of the most effective methods for allowing a machine to learn various levels of data properties (e.g., images). The success of every intelligent machine learning algorithm is determined by its features. Clustering algorithms are unsupervised machine-learning algorithms that collect data based on their similarity such as FCM.

C. Proposed System

In this work, we applied the FCM algorithm to deal with the burn area, the burn area is labeled as "white" and the background is marked as "black" in a binary image if the body part outline detection results are accurate. Fig. 5 shows the flow diagram of the suggested system. The system first

converts the input image into a gray image and then entered into the FCM algorithm to segment the injured area, after that an identification of the burn area is obtained. Fig. 5 shows the flow of the steps.

Fig. 6 shows the stages of the proposed system, which mainly consists of three stages: The first stage: is the stage that includes input image, and then converting the picture into a gray color system to facilitate the correct extraction of data. In this work, second and third-degree burns to the skin are taken into consideration.

The second stage: It is the stage through which the data used from the first stage is entered into the directed deep

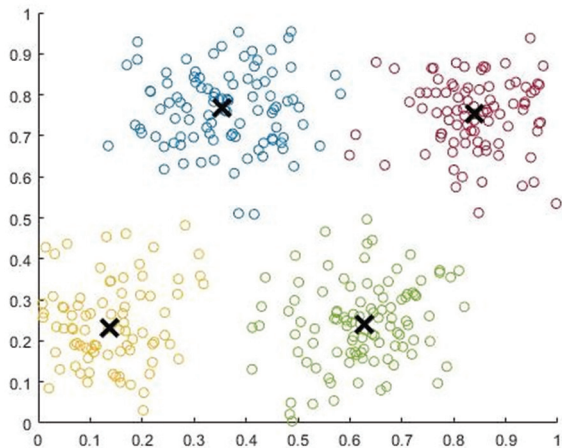


Fig. 4. Fuzzy c-means clustering algorithm. Each cluster's data points are represented by a different color. Each cluster's center is represented with a black X.

learning algorithm, and through it, the infected part is separated from the healthy part to be transferred to the third stage, which is the stage of data extraction for diagnosis to help the doctor expedite the process processing. Fig. 7 explains the details of the deep layers with fuzzy clustering for each layer until we reach the final result. Fig. 7 demonstrates that the framework contains three parts. The input burn image part, and the image. The second part is the proposal network that extracts the regions of interest, and the third part is the network that output result.

IV. EXPERIMENTAL RESULTS

First, the used database included real burn images under hospital conditions that contain superficial and full-thickness burns, and some input images are from Google search as well. Manual input images, and (Stephen, 2020) database has also been used in our work.

The initial number of segments of the burn images under consideration is determined by experimental results and it decided to set up at 2 clusters in which the required result is to detect the burned area from the unbury areas, as shown in Table I.

System performance measures could be investigated by several parameters. In this work, two sets of metrics are taken into consideration to evaluate the accuracy of the suggested method, the first metric is sensitivity, precision, accuracy, and precision, and the second metric is a calculating mean square error (MSE), and peak sign to noise ratio (PSNR).

Sensitivity and precision were used as performance measures for burn categorization Sensitivity is the rate



Fig. 5. Block diagram of the proposed system.

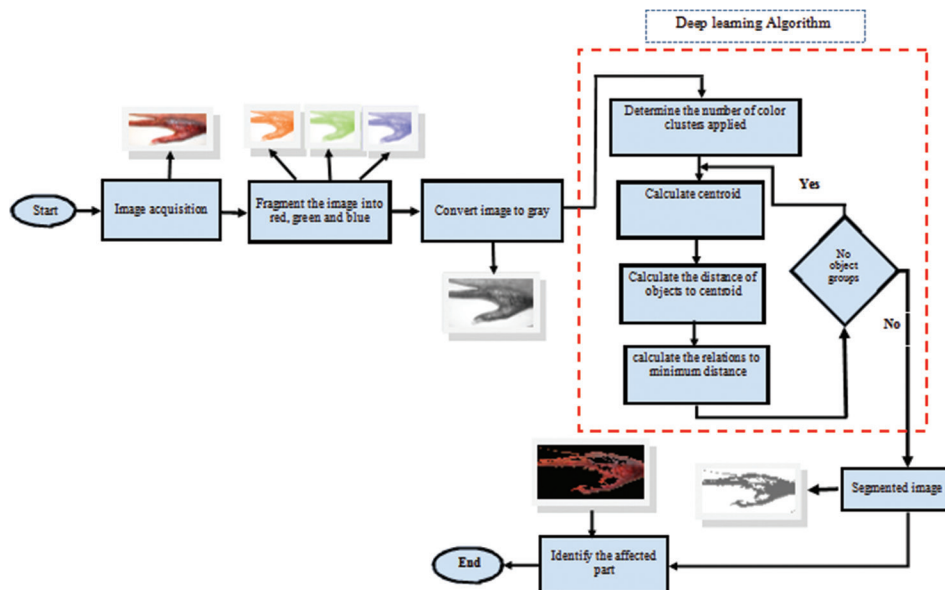


Fig. 6. System flow diagram.

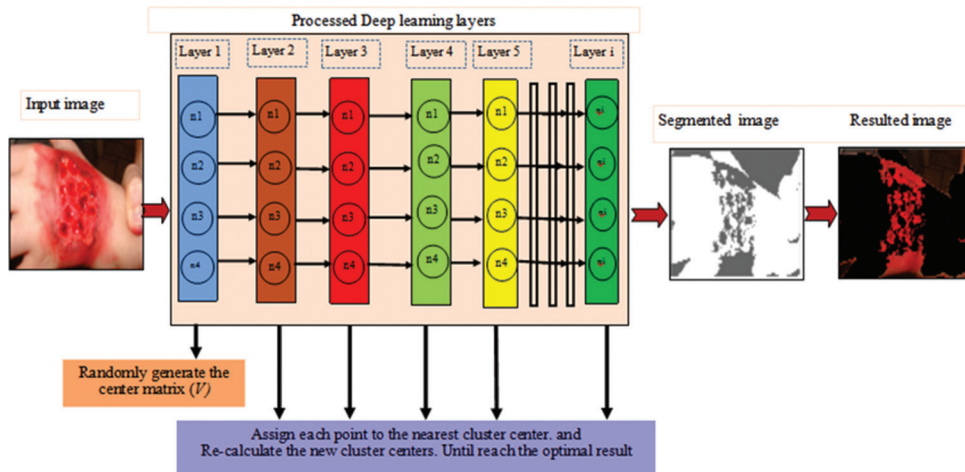


Fig. 7. Graphical representation of deep learning fuzzy c-means layers proposed.

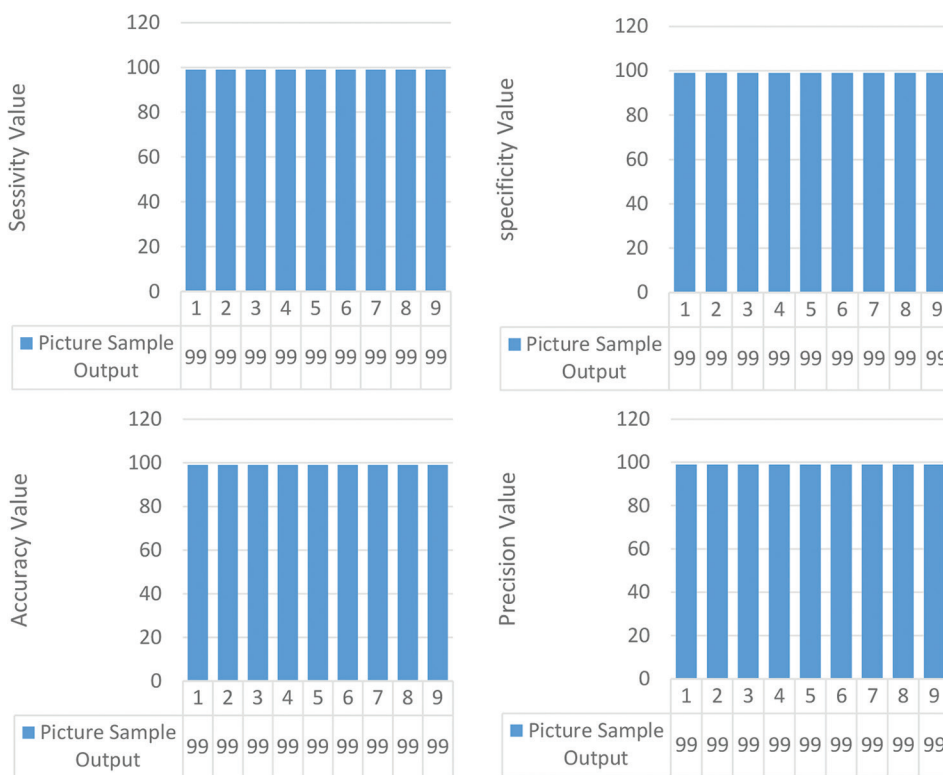


Fig. 8. Performance metric representation, sensitivity, specificity, accuracy, and precision.

TABLE I
INITIAL ESTIMATES OF K





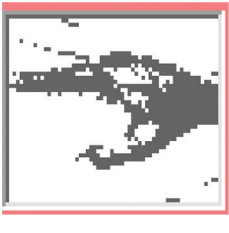
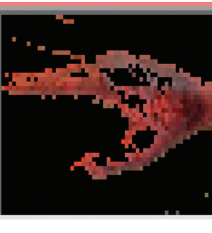




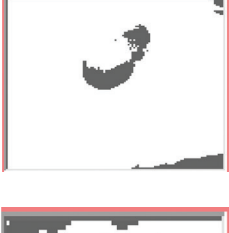



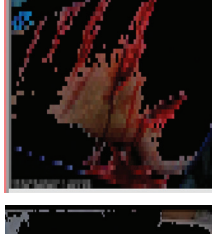


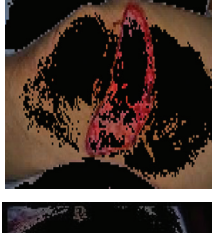

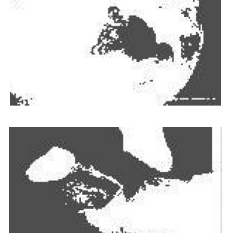
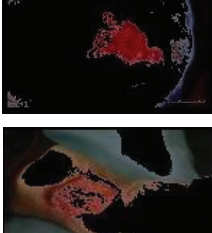



Input image	Estimation of K
All input images	2

TABLE II
PERFORMANCE METRIC REPRESENTATION, AS SENSITIVITY, SPECIFICITY, ACCURACY, AND PRECISION FOR SOME BURN IMAGES

Image No.	Sensitivity	Specificity	Accuracy	Precision
1	63	99	70	99
2	55	98	59	99
3	61	99	67	99
4	51	90	51	99
5	64	99	72	99
6	60	99	67	99
7	58	98	64	99
8	59	99	65	99
9	65	98	61	99

of correctly classifying a burn, sensitivity = $TP/(TP + FN)$; where true positives (TP) are burns images correctly identified, false negatives (FN) are burns wrongly classified. The other performance metric was precision, which is the rate of correctly detected burns, precision = $TP/(TP + FP)$; where false positives (FP) are the area that has been wrongly labeled as burns such as in the darkened skin case, besides

TABLE III
RESULTS OF APPLYING DEEP FUZZY C-MEANS ON SOME BURN IMAGES

Image No.	Original image	Segmented image	Resulted image
1			
2			
3			
4			
5			
6			
7			
8			

(Contd...)

TABLE III
(CONTINUED)




Image No.	Original image	Segmented image	Resulted image
9			

TABLE IV
MSE AND PSNR PERFORMANCE MEASURE FOR THE SEGMENTED IMAGE

Image No.	MSE	PSNR
1	52.2266	39.5413
2	38.8464	40.1840
3	46.0421	39.8150
4	30.6418	40.6992
5	51.5427	39.5699
6	45.8580	39.8237

TABLE V
MSE AND PSNR PERFORMANCE MEASURE FOR THE RESULTED IMAGE

Image No.	MSE	PSNR
1	49.2013	39.6709
2	37.103	40.2837
3	46.2525	39.8051
4	29.9125	40.7515
5	49.3238	39.6655
6	45.1898	39.8555

accuracy, specificity metrics, where accuracy = (TP + TN)/(TP + TN + FP + FN), and specificity = TN/(TN + FP) as shown in Table II. Where the first column represents the number of images.

The accuracy of the system is considered as the maximum accuracy achieved in the system, which is approximately to 75%. In Fig. 8, the four evaluation metrics are depicted for details clarifying.

While the second metric, MSE is used to measure the error between the original input image and the processed image. MSE between two different images such as $g(x, y)$ and $\hat{g}(x, y)$ is defined as in equation (7):

$$MSE = \frac{1}{MN} \sum_{n=0}^M \sum_{m=0}^N [\hat{g}(n, m) - g(n, m)]^2 \quad (7)$$

Sign to noise ratio is a designing term for the power proportion between a sign (significant data) and the background noise as in equation (8):

$$SNR = \left[\frac{\sum_{i=0}^{N-1} w_i^2}{MSE} \right] \quad (8)$$

The PSNR addresses the proportion between the peak signal and the mean square mistake, usually calculated to evaluate the objective quality of the processed image after

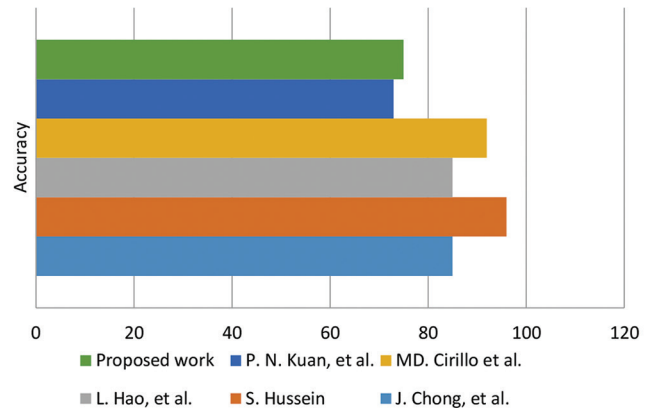


Fig. 9. Accuracy of different approaches.

performing the segmentation process, and it is determined by the equation (9):

$$PSNR(dB) = 10 \log_{10} \left[\frac{255^2}{MSE} \right] \quad (9)$$

Typically, PSNR value range from 20 to 40, and they are usually reported up to two decimal points. The actual value is not meaningful, but the image segmentation between the two values for different reconstructed images gives more indications about the quality (Chong, et al., 2019; Umme, Morium and Mohammed, 2019).

Table III shows the segmentation result of the proposed segmentation method for some burn images. The first column represents the original burn image, the second column represents the segmentation result using the deep FCM technique, and the third column represents the segmentation result.

Tables IV and V show the calculation of MSE and PSNR performance measure for the segmented image, and resulted image, respectively.

The categorization of the previously discussed state-of-the-art research in terms of scope of the system, frameworks used, applied techniques, dataset utilized, training and evaluating the number of images, and accuracy, as explained in Table VI.

To evaluate the performance of the proposed method, we compare the segmentation results achieved with our method, Table VII introduces a comparison of the proposed work and some other methods in terms of accuracy, whereas Fig. 8 shows the graphical representation of Table VII.

TABLE VI
COMPARATIVE ANALYSIS OF DIFFERENT RELATED WORKS RESEARCHES

Author name	Scope of the system	Frameworks used	Applied techniques	Data set	Training/Evaluating	Accuracy
Chong, et al.	Classification of burn images	Segmenting burn images	Convolutional neural network (Mask R-CNN)	Common Objects in Context (COCO) data set	1000 burn images for training and 150 for evaluating	84.51%
Badea, et al.	Classification of burn images	Identification of burn areas image patches	Convolutional neural network	Manual dataset, total 611 images depicting burn wounds.	The training and validation sets contain a total of 74763 patches of different images	75.91%
Prabhakar, Gauraveand and Kailesh	Classification of images with color loss	Segmenting of burn photos	Mask Regions of the R-CNN	Wuhan Hospital Burn Department, used own smartphone to collect fresh burn injuries	1000 burn pictures for training and another 150 for assessment	84.5%
Brenda, and Roberto	Classification of burn images	identification and classification of burns images	dictionary learning accompanied by K-singular value decomposition	Public websites	Dictionaries without K-SVD training (L= 1, 2, 3), or K-SVD-trained dictionaries with 30 iterations and various factor values (L= 1, 2, 3) for testing	90%
Murfi, Rosaline and Hariadi	Topic detection for textual data	Topic detection method that combines deep auto encoder (DAE) for representation learning and FCM for fuzzy clustering	Deep auto encoder and fuzzy c-means	Enron – an English email dataset. The first dataset is Enron consisting of 500,000 emails generated by employees of the Enron Corporation	Use pre-trained word2vec model trained on the Google News dataset for the English email dataset/The model contains 300-dimensional vectors for 3 million words and phrases	N/A
				Berita – An Indonesian news dataset. consisting of 50,304 digital Indonesian news articles shared online	Construct the word2vec model using a corpus consisting of 750,000 Indonesian documents from wiki, news, and tweets	
Kuan, et al.	Classification of burn injury images.	both Discrete wavelet transform (DWT) and principle component analysis (PCA), Gray Level Co-occurrence Matrix (GLCM) method	the Waikato Environment for Knowledge Analysis (WEKA)	Both the supplied test set and 10-fold cross validation methods	The dataset splitting into two sets, 70% and 30% for training and testing, respectively	73.2%
Hussein	Segmentation of mammalian body skin (Mice)	Segmenting mice skin layers from images into epidermis, dermis, and adipose layers	Combined color deconvolution method with fuzzy C-mean (FCM) clustering	A dataset of 7,000 mice skin images taken at $\times 20$ magnification	100 images were randomly selected from 1,000 images.	96%
Wang, et al.	Classification of burn images.	A convolutional neural network (CNN), MobileNetV219	Deep convolutional neural networks	The foot ulcer dataset	Training set containing 3645 images and a testing set containing 405 images	90.47%
Despo, et al.	Classification of burn images.	Predicting different burn depths	Applied FCN with a CRF layer	749 images from the Santa Clara Valley Medical Center and 180 images from Google search to create BURNED dataset	334 out of the 396 images in the training set, testing set is 62 images	N/A
Hao, et al.	Segmentation and diagnosis of burn images.	Deep learning used to automate segmentation of burn area and diagnosis.	Fully convolutional Networks	Jianggan District Hospital, Hangzhou. no. of burn images is 1200	960 images are used for training the model and 240 images for testing.	85%
Cirillo, et al.	Segmentation and diagnosis of burn images.	Used burn-depth assessment using semantic segmentation	Convolutional neural network, based on the U-Net	100 burn images	17 images to train the network, and 83 images to evaluate the network.	92%

TABLE VII
COMPARISON OF THE PROPOSED WORK AND SOME OTHER METHODS IN TERM OF ACCURACY

Author names	Accuracy
Chong, et al.	84.51%
Hussein	96%
Hao, et al.	85%
Cirillo, et al.	92%
Kuan, et al.	73.2%
Proposed work	75%

From Fig. 9, we can notice that despite the benefits of using an autonomous wound detection stage preceding the segmentation has its advantages, cases of erroneous wound detection must also be taken into consideration.

IV. CONCLUSION

Image segmentation is regarded as a crucial stage in the processing of images. One of the popular techniques for

segmenting images is the clustering algorithm. However, there are problems with this approach, including sensitivity to initial parameters, getting stuck in local optima, and being unable to identify among objects with identical luminescence. This research proposed a deep learning based FCM approach to detect the injured area. Experimental results showed that the proposed technique is simple, and effective in the real input image. Two types of metrics have been used to evaluate the system, and a comparison with various types of research is also presented to examine our system correctly. Our future work is to develop the work by combining other machine learning algorithms with this system to classify the degree of burn as superficial, partial thickness, or full thickness.

V. ACKNOWLEDGMENT

We would like to express our gratitude for the reviewers' efforts in reading and commenting on our paper. A great thanks my colleagues, for their patient instruction, passionate support, and constructive criticisms of this study effort.

REFERENCES

- Alcala-Fdez, J. and Alonso, J.M., 2016. A survey of fuzzy systems software: Taxonomy, current research trends and prospects. *IEEE Transactions on Fuzzy Systems*, 24(1), pp.40-56.
- Badea, M.S., Vertan, C., Florea, C., Florea, L. and Bădoiu, S., 2016. Automatic Burn Area Identification in Color Images. In: *2016 International Conference on Communications (COMM)*. pp.65-68.
- Badrinarayanan, V., Kendall, A. and Cipolla, R., 2017. SegNet: A deep convolutional encoder-decoder architecture for image segmentation. *IEEE Transactions on Pattern Analysis and Machine Intelligence*, 39(12), pp.2481-2495.
- Bekir, K., 2016. The positive effects of fuzzy C-means clustering on supervised learning classifiers. *International Journal of Artificial Intelligence and Expert Systems*, 7(1), pp.1-8.
- Bezdek, J.C., 1981. *Pattern Recognition with Fuzzy Objective Function Algorithms*. Plenum Press, New York.
- Brenda, R.O. and Roberto, R.R., 2021. Detection and classification of burnt skin via sparse representation of signals by over-redundant dictionaries. *Computers in Biology and Medicine*, 132, p.104310.
- Chong, J., Kehua, S., Weiguo, X. and Ziqing, Y., 2019. Burn image segmentation based on mask regions with convolutional neural network deep learning framework: More accurate and more convenient. *Burns and Trauma*, 7, p.6.
- Cirillo, M.D., Mirdell, R., Sjöberg, F. and Pham, T.D., 2021. Improving burn depth assessment for pediatric scalds by AI based on semantic segmentation of polarized light photography images. *Burns*, 47(7), pp.1586-1593.
- Deepak, L., Antony, J. and Niranjan, U.C., 2012. Hardware Co-simulation of Skin Burn Image Analysis. In: *19th IEEE International Conference in High Performance Computing (HiPC-2012)*.
- Despo, O., Yeung, S., Jopling, J., Pridgen, B., Shekter, C., Silberstein, S., Fei-Fei, L. and Milstein, A., 2017. *BURNED: Towards Efficient and Accurate Burn Prognosis Using Deep Learning*. Available from: <http://cs231n.stanford.edu/reports/2017/pdfs/507.pdf> [Last accessed on 2022 Feb 01].
- Domagoj, M. and Damir, F., 2020. A systematic overview of recent methods for non-contact chronic wound analysis. *Applied Science*, 10, p.7613.
- Fangzhao, L., Changjian, W., Xiaohui, L., Yuxing, P. and Shiyao, J., 2018. A composite model of wound segmentation based on traditional methods and deep neural networks. *Computational Intelligence and Neuroscience*, 2018, p.4149103.
- Hansen, G.L., Sparrow, E.M., Kokate, J.Y., Leland, K.J. and Iaizzo, P.A., 1997. Wound status evaluation using color image processing. *IEEE Transactions on Medical Imaging*, 16(1), pp.78-86.
- Hao, L., Kepiang, Y., Siyi, C., Wenjun, L. and Zhihui, F., 2021. A framework for automatic burn image segmentation and burn depth diagnosis using deep learning. *Computational and Mathematical Methods in Medicine*, 2021, p. 5514224.
- Hasan, M.M., Ibraheem, N.A. and Abdulhadi, N.M., 2022. 2D geometric object shapes detection and classification. *Webology*, 19(1), pp.1689-1702.
- Health Encyclopedia Site. Available from: <https://www.urmc.rochester.edu/encyclopedia/content.aspx?ContentTypeID=90&ContentID=P09575> [Last accessed on 2022 Oct 01].
- Hussein, S., 2021. Automatic layer segmentation in H&E images of mice skin based on colour deconvolution and fuzzy C-mean clustering. *Informatics in Medicine Unlocked*, 25, p.100692.
- Kuan, P.N., Chua, S., Safawi, E.B., Wang, H.H. and Tiong, W., 2018. A comparative study of the classification of skin burn depth in human. *Journal of Telecommunication Electronic and Computer Engineering*, 9(2-10), pp.15-23.
- Liangrui, P., Zhichao, F. and Shaoliang, P., 2022. A review of machine learning approaches, challenges and prospects for computational tumor pathology. *arXiv*, 2206, p.01728.
- Liu, X., Song, L., Liu, S. and Zhang, Y., 2021. A review of deep-learning-based medical image segmentation methods. *Sustainability*, 13(3), p.1224.
- Malini, S., Siva, K. and Niranjan, U., 2013. Classification methods of skin burn images. *International Journal of Computer Science and Information Technology*, 5(1), pp.109-118.
- Miller, S.J., Burke, E.M., Rader, M.D., Coulombe, P.A., and Lavker, R.M., 1998. Reepithelialization of porcine skin by the sweat apparatus. *The Journal of Investigative Dermatology*, 110(1), pp.13-19.
- Murfi, H., Rosaline, N. and Hariadi, N., 2022. Deep autoencoder-based fuzzy c-means for topic detection. *Array*, 13, p.100124.
- Nameirakpam, D., Khumanthem, M. and Yambem, J.C., 2015. Image segmentation using K-means clustering algorithm and subtractive clustering algorithm. *Procedia Computer Science*, 54, pp.764-771.
- Papini, R., 2004. Management of burn injuries of various depths. *British Medical Journal*, 329(7458), pp. 158-160.
- Prabhakar, K., Gaurave, S. and Kailesh, P., 2020. Burn image segmentation based on mask regions with convolutional neural network deep learning framework. *International Journal of Research in Engineering Science and Management*, 3(8), pp.478-482.
- Rahman, T. and Islam, M.S., 2021. Image Segmentation Based on Fuzzy C Means Clustering Algorithm and Morphological Reconstruction. In: *International Conference on Information and Communication Technology for Sustainable Development (ICICT4SD)*. pp.259-263.
- Sabeena, B. and Rajkumar, P., 2019. Diagnosis and detection of skin burn analysis segmentation in colour skin images. *International Journal of Advanced Research in Computer and Communication Engineering*, 6(2), pp. 369-374.
- Stephen, T., 2020. Stock Pictures of Wounds. Medetec Wound Database. Available from: <https://www.medetec.co.uk/files/medetec-image-databases.html> [Last accessed on 2022 Feb 01].
- Tina, M., Uros, M., Karin, S.K., Raščan, I.M. and Dragica, M.S., 2015. Advanced therapies of skin injuries. *Wiener Klinische Wochenschrift*, 127(5), pp.187-198.
- Ugur, U.K., Erdiñç, K., Tolga, B., Yesim, A. and Serder, T., 2019. Automatic classification of skin burn colour images using texture-based feature extraction. *IET Image Processing*, 13(11), pp.2018-2028.
- Umme, S., Morium, A. and Mohammed, S.U., 2019. Image quality assessment through FSIM, SSIM, MSE and PSNR-a comparative study. *Journal of Computer*

and *Communications*, 7(3), pp.8-18.

Wagh, A., Jain, S., Mukherjee, A., Agu, E., Pedersen, P.C., Strong, D., Tulu, B. Lindsay, C. and Liu, Z., 2020. Semantic segmentation of smartphone wound images: Comparative analysis of AHRF and CNN-based approaches. *IEEE Access*, 8, pp.181590-181604.

Wang, C., Anisuzzaman, D.M., Williamson, V., Mrinal, K.D., Behrouz, R., Jeffrey, G., Sandeep, G. and Zeyen, Y., 2020. Fully automatic wound segmentation

with deep convolutional neural networks. *Scientific Reports*, 10(1), p.21897.

Wang, C., Pedrycz, W., Li, Z. and Zhou, M., 2021. Residual-driven fuzzy C-means clustering for image segmentation. *IEEE/CAA Journal of Automatica Sinica*, 8(4), pp.876-889.

Yeganejou, M. and Dick, S., 2018. Classification Via Deep Fuzzy C-means Clustering. In: *IEEE International Conference on Fuzzy Systems (FUZZ-IEEE)*, 2018. pp.1-6.